External Grant Award Nos. 08HQGR0032, 08HQGR0039, 08HQGR0042 and 08HQGR0045

DEVELOPMENT OF A CALIFORNIA-WIDE THREE-DIMENSIONAL SEISMIC WAVESPEED MODEL: COLLABORATIVE RESEARCH WITH UW-MADISON, LDEO/COLUMBIA UNIV., U. C. SAN DIEGO, AND CALTECH

Clifford H. Thurber
Geology and Geophysics, University of Wisconsin-Madison
1215 W. Dayton St.
Madison, WI 53706
Telephone: (608) 262-6027
FAX: (608) 262-0693
Email: thurber@geology.wisc.edu

Peter M. Shearer
IGPP 0225, University of California San Diego
La Jolla, CA 92093-0225
Telephone: (858) 534-2260
FAX: (858) 534-5332
Email: pshearer@ucsd.edu

Felix Waldhauser
Lamont-Doherty Earth Observatory, Columbia University
P.O. Box 1000, Palisades, NY 10964
Telephone: (845) 365-8538
FAX: (845) 365-8150
Email: felixw@ldeo.columbia.edu

Egill Hauksson
California Institute of Technology
Mail code 251-21, 1200E California Blvd.
Pasadena, CA 91125
Telephone: 626-395-6954
FAX: 626-564-0715
Email: hauksson@gps.caltech.edu

External Grant Award Nos. 08HQGR0032, 08HQGR0039, 08HQGR0042 and 08HQGR0045

DEVELOPMENT OF A CALIFORNIA-WIDE THREE-DIMENSIONAL SEISMIC WAVESPEED MODEL: COLLABORATIVE RESEARCH WITH UW-MADISON, LDEO/COLUMBIA UNIV., U. C. SAN DIEGO, AND CALTECH

Clifford H. Thurber
Geology & Geophysics, Univ. of Wisconsin-Madison, 1215 W. Dayton St., Madison, WI 53706
Telephone: (608) 262-6027, FAX: (608) 262-0693
Email: thurber@geology.wisc.edu

Peter M. Shearer
IGPP 0225, University of California San Diego, La Jolla, CA 92093-0225
Telephone: (858) 534-2260, FAX: (858) 534-5332
Email: pshearer@ucsd.edu

Felix Waldhauser
Lamont-Doherty Earth Observatory, Columbia University, P.O. Box 1000, Palisades, NY 10964
Telephone: (845) 365-8538, FAX: (845) 365-8150
Email: felixw@ldeo.columbia.edu

Egill Hauksson
California Inst. Technology, Mail code 251-21, 1200E California Blvd., Pasadena, CA 91125
Telephone: 626-395-6954, FAX: 626-564-0715
Email: hauksson@gps.caltech.edu

Abstract

We have developed a statewide, three-dimensional (3D) tomographic model of the P- and S-wave velocity structure of the crust and uppermost mantle of California. The dataset combines first arrival times from earthquakes and identified quarry blasts recorded on regional network stations, and travel times of first arrivals from explosions and airgun blasts recorded on profile receivers and network stations. The model is obtained by using a regional-scale double-difference tomography algorithm, which incorporates a finite-difference travel time calculator and spatial smoothing constraints. This algorithm is designed to solve jointly for 3D velocity structure and earthquake locations using both first arrival times and differential times, leading to improved resolution in the seismically active areas where the differential data provide dense sampling. Our model is able to image the principal features present in previous separate regional models for northern and southern California, such as the high-velocity subducting Gorda Plate, upper-crustal velocity highs beneath the Sierra Nevada and much of the Coast Ranges, low velocities of the Great Valley, Ventura Basin, Los Angeles Basin, and Imperial Valley, and a high-velocity body in the middle to lower crust underlying the Great Valley. The new statewide model has improved areal coverage compared to previous models, and also extends to greater depth due to the inclusion of substantial data at large epicentral distances. This model can be applied to a variety of regional-scale studies in California, such as providing a preliminary unified statewide earthquake location catalog and regional waveform modeling.

Project Results

We report on our development of the first statewide three-dimensional (3D) seismic velocity model for California based on regional earthquake and explosion arrival time data. The collaborative project involves four university institutions, UW-Madison, LDEO/Columbia Univ., U. C. San Diego, and Caltech, and is coordinated with USGS internal projects.

The data sets for our Vp model are the first-arrival absolute and differential times of 8720 earthquakes recorded by the seismic networks in California, consisting of 4325 events from the Northern California Seismic Network, 3668 events from the Southern California Seismic Network and 727 events from the Pacific Gas and Electric seismic network (blue, pink, and green dots in Figure 2a, respectively). These earthquakes were selected based on having the greatest number of P picks among those events within a 6 km radius, with a magnitude threshold of 2.5. The total number of P picks in our data set is 551,318 with an average of 63 picks per event. In order to improve constraints on the shallow crustal structure, we assembled first arrival times from 3110 explosions and airguns (red circles in Figure 2b) recorded on profile receivers and network stations. The principal active-source data sets and sources are listed in Table 2. Quarry blasts, which have known locations but unknown origin times, are also valuable to include in tomographic inversions because they provide constraints that are almost as good as the active-source data. We include data from 44 quarry blasts (blue circles in Figure 2b), with 19 in southern California (see Lin et al., 2007) and 25 in northern California. Figure 2c shows the locations of temporary and network stations used in our study.

The model is obtained by using a regional-scale DD tomography algorithm (tomoFDD; Zhang and Thurber, 2006), which maps a spherical-Earth coordinate system into a Cartesian coordinate system (a "sphere in a box"; Flanagan et al., 2007) and incorporates a finite-difference travel time calculator and spatial smoothing constraints. This5 algorithm is designed to solve jointly for 3D velocity structure and earthquake locations using both first arrival times and differential times, leading to improved resolution in the seismically active areas where the differential data provide dense sampling.

3D Coarse Model

Because of the large spatial scale and amount of data in our study, we first solve for a coarse 3D Vp model starting with a one-dimensional (1D) velocity model (shown in the small panel of Figure 2d) for the entire state. This 1D model is based on standard regional 1D velocity models used to locate earthquakes by the seismic networks in northern and southern California. The starting model nodes (shown in Figure 2d) are uniformly spaced at 30 km intervals in the horizontal directions and extend 570 km in the SW-NE direction and 1320 km in the NW-SE direction. In the vertical direction, the nodes are positioned at -1, 1, 4, 8, 14, 20, 27, 35 and 45 km (relative to mean sea level). We only use absolute arrival times for this 3D coarse model. An a priori Moho is not included at this stage, but is introduced later for the finer-scale model. Preliminary inversions were carried out using the tomography algorithm simul2000 (Thurber and Eberhart-Phillips, 1999). This algorithm simultaneously solves for 3D velocity structure and earthquake locations using the first arrival times employing an iterative damped-least-squares method. This step was taken for data quality control purposes (i.e., identifying poorly constrained events and picks with very high residuals) and to provide formal but approximate estimates of velocity model resolution and uncertainty. After the data quality control step using simul2000, we applied the regional-scale DD tomography algorithm, which is more suitable for the large-scale area in this study. The smoothing constraint weighting of 100 and the damping

parameter of 350 were chosen by examining the data variance versus model variance trade-off curves.

3D Starting Model Adjustments

After we obtain the 3D coarse velocity model, we introduce an a priori Moho interface modified from the results of Fuis and Mooney (1990). We set the velocity to 8 km/s in the model layer right below the Moho and include a reasonable gradient with depth for deeper layers. In order to start with a conservative 3D model, we removed the low velocity anomalies in the 3D coarse model, i.e., we require that velocity is initially a monotonically increasing function of depth. The resulting adjusted 3D model is the starting model for our final P velocity model. Figure 3a shows the map view of this model at 4 km depth, with the layer-average velocity values in the inset.

In order to use differential times to obtain a finer-scale model given our computer memory limitations, we split the entire state into 5 subregions (Figure 3a). The adjacent subregions overlap by about 30 km. We use the same depth layers as the coarse model. Figure 3b shows the event and station distributions for subregion 1 as an example. For each subregion inversion, we use absolute and differential times from events inside the subregion (blue circles in Figure 3b) that are recorded by all the stations (black triangles) and only absolute times from events outside of the subregion (pink circles) that are recorded by stations inside of the subregion. In this way, we improved the resolution of the resulting velocity model for the deeper layers due to the inclusion of substantial data at large epicentral distances. We also include all available explosion and quarry data for each subregion (red stars). Inside of each subregion, the horizontal nodes are spaced at a 10 km interval in the areas with dense data coverage and 20 km in other areas (yellow squares). The node spacing outside of each subregion is 30 km (green squares). The initial velocity value at each node is computed from the velocity values at the surrounding eight nodes of the coarse initial model using tri-linear interpolation as described in Thurber and Eberhart-Phillips (1999). The velocities outside of each subregion are fixed during the inversion of the inside-subregion velocities. Our final statewide velocity model is a stitched version of all the 5 subregion models.

Quality and Resolution

The quality of our model can be evaluated by its ability to (1) fit the observed arrival time data and (2) produce accurate locations for on-land controlled-source explosions, which have known coordinates. Figure 4 shows a comparison of the arrival time residual distribution before (a) and after the coarse (b) and final (stitched) (c) 3D velocity inversions. The root-mean-square misfit is reduced by over a factor of 3, from 1.35 s to 0.38 s, after the 3D coarse model inversion, and then to 0.25 s after the final model inversion. Note that most of the improvement of arrival time fit after the 3D final model inversion is mainly due to the lower differential time residuals; the fit of the absolute times is only slightly better than that after the 3D coarse model inversion.

We independently located the on-shore explosions using the starting 1D and the coarse and final 3D velocity models and then calculated the horizontal and vertical location differences between the relocations and the known true locations. Figure 5 shows histograms of shot location accuracy relocated using the starting 1D model compared to the two 3D models for both horizontal and vertical coordinates. The horizontal location errors are all positive; the vertical errors are positive when the assigned location is deeper than the true location and negative when the assigned location is shallower than the true location. For the 1D model, the error distributions

are quite broad, with a mean error of 1.23 km, and a standard deviation of 1.08 km horizontally. The vertical error distribution has peaks at about 0.6 and 4.5 km, a mean (absolute) error of 2.19 km, and a standard deviation of 2.38 km. In contrast, the 3D coarse model error distributions are peaked between 0 and 1 km, with mean errors of 0.60 and 0.32 km and standard deviations of 0.59 and 0.82 km for the horizontal and vertical errors, respectively. Although this model is coarse, the 3D shot relocations are significantly improved, especially in depth. This is because a single 1D velocity model cannot account for lateral heterogeneity in velocity structure across all of California. Further, the 3D final model location error distributions are peaked around 0.2 km, with mean errors of 0.35 and 0.15 km and standard deviations of 0.39 and 0.41 km for the horizontal and vertical errors, respectively. The reduction in relocation errors of about a factor of 2 over the 3D coarse model indicates that our final model significantly improves resolution for the lateral heterogeneities in the 3D velocity structure, especially at shallow depths.

To assess the model quality, we performed a restoration and a checkerboard resolution test similar to those in Thurber et al. (2009). In the restoration test, event hypocenters, station locations and synthetic travel times, calculated from the final inverted model, have the same distribution as the real data. We followed the same inversion strategies as those for the real data and the inverted final model is similar to the true model. Recovery problems occur mainly around the model edges, including around the Moho. In the checkerboard test, the synthetic times are computed through the 1D starting velocity model with ±5% velocity anomalies across two grid nodes. Except in the shallowest and deepest layers and the model edges, the checkerboard recovery is reasonably good.

Final P-wave Velocity Model

Figure 6 shows map view slices through the resulting tomographic P velocity model. Pink dots in each figure represent earthquakes relocated within ±1 km of each layer depth. The white contours enclose the areas where the derivative weight sum (DWS; Thurber and Eberhart-Phillips, 1999) is greater than 50. DWS measures the sampling of each node and serves as an approximate measure of resolution (Zhang and Thurber, 2007). Areas with DWS value above 50 correspond well to resolved areas in the synthetic tests.

Figure 6a and 6b show the P-wave velocities in the top two layers of our model. The average velocity values are 4.91 km/s at 1 km and 5.67 km/s at 4 km depth. The velocities in these shallow layers generally correlate with the surface geology. Lower values are observed in basin and valley areas, such as the Great Valley, Southern San Joaquin Valley, Ventura Basin, Los Angeles Basin, and Imperial Valley, whereas relatively higher velocities are present in the mountain ranges, such as the northern Coast Ranges, Transverse Ranges, Peninsular Ranges, and Sierra Nevada. The lowest velocity anomalies (about 2.9 km/s) appear in the Great Valley and southern San Joaquin Valley. However, these low anomalies are at the edge of our well-resolved areas because of the sparse event distribution in this region. Fairly high velocity anomalies (~6.0 km/s) at 1 km depth in the Klamath Mountains and Mount Shasta area are observed that are consistent with the results from seismic-refraction and gravity data in this area (Zucca et al., 1986; Fuis et al., 1987), but are not seen in the recent northern California P-wave velocity model by Thurber et al. (2009). This high velocity body extends to 14 km depth in our model, reaching ~6.5-6.7 km/s at 4 km, ~6.7-7.1 km/s at 8 km, and ~7.0-7.1 km/s at 14 km depth, with relatively little structural variations along the north-south direction. These velocities are consistent with the conclusion in Fuis et al. (1987) who claimed that an imbricated stack of oceanic rock layers underlies the Klamath Mountains. Another high velocity anomaly zone is apparent at 1 and 4 km

depth in the Lake Oroville area. The ~6.8 km/s velocity at 4 km depth is generally consistent with the observations by Spieth et al. (1981) that the velocity is of the order of 7.0 km/s at a depth of 5 km. This high velocity anomaly (~6.9 km/s) extends to 8 km depth in our model. The high velocities at 1 km depth in the southern Sierra Nevada area, ranging from 5.2 km/s to 5.8 km/s, are consistent with the results of Fliedner et al. (1996, 2000). The velocities at 4 km depth are generally higher than those estimated by Thurber et al. (2009) (~6.0 km/s compared to ~5.3 km/s), and our model is more consistent with the results based on active seismic refraction experiment by Fliedner et al. (1996, 2000).

In southern California, near-surface velocities are also relatively high in the western Mojave Desert. The anomalies are slightly higher than previous results (e.g., Hauksson, 2000; Lin et al., 2007). We think this may be due to the inclusion of the active-source data in this area, which were not used before. In the Imperial Valley area, the slowest velocity at 1 km depth is 3.07 km/s in our model, but it is about 3.6 km/s at the surface in Lin et al. (2007). The latter concluded that their model slightly overestimates the near-surface velocity compared to seismic refraction results (Fuis et al., 1984). The reduction of this overestimation indicates that our model has better resolution for near-surface structure. The southern San Joaquin Valley is better resolved in this new model, which is at the northern boundary of the study area in Lin et al. (2007).

Figure 6c and 6d show map views for 8 and 14 km depths, with average velocity values of 6.13 km/s and 6.47 km/s, respectively. These layers are the two best-resolved layers in our model because of the abundant seismicity at these depths, and the results are generally quite compatible with previous tomographic results. At 8 km depth, a strong velocity contrast is apparent between the Great Valley and the Sierra Nevada. At 14 km depth, some of the features we see in the shallow layers are reversed, i.e., the basin and valley areas show relatively high velocity anomalies and lower values are present under the mountain ranges. The reversal of the velocity anomalies associated with most of the major basins is also observed in previous southern and northern California tomography studies (Lin et al., 2007; Thurber et al., 2009). Generally, the velocity anomalies in well-resolved areas are consistent with the separate southern and northern California velocity models of Lin et al. (2007) and Thurber et al. (2009), although for these two layers, the velocities in the northern Coast Ranges are slightly lower (~5%) than what is observed in the Thurber et al. (2009) model. Map views for the 20 and 27 km depth layers are shown in Figure 6e and 6f, with average velocity values of 6.86 km/s and 7.33 km/s, respectively. The resolution of the southern California model by Lin et al. (2007) is poor below 17 km depth, so we focus on the comparison in northern California. At 20 km depth, the model is consistent with the results of but is slightly slower in the center of the Great Valley. At 27 km depth, the Sierra Nevada area shows about 6.0 km/s low velocity anomalies, but in the same area, the velocity in Thurber et al. (2009) is about 6.5 km/s. Our model extends to 45 km depth. Figure 6g and 6h show the map views of the last two layers at 35 km and 45 km depths. Although the model is not resolved nearly as well as the shallower layers, we are able to see the low velocity anomalies in the Sierra Nevada region.

Because of the large scale in our study area, we only present three cross-sections through our model here. One is parallel to the San Andreas fault (SAF; X=0 km in the Cartesian coordinate system), and the other two are perpendicular to the SAF (Y=210 km and Y=-30). In Figure 7 we show the velocity cross-sections through the resulting model along the three profiles whose locations are shown in Figure 1.

The X = 0 km section in Figure 7a starts in the northern Coast Ranges where intermediate velocities (Vp < 6.2 km/s) extend into the lower crust. At depths greater than 20 km, the seismicity and high velocities of the subducting Gorda Plate are visible. From Y ~ 350 to -210 km, the low near-surface velocities of the Great Valley and Southern San Joaquin Valley sediments and sedimentary rocks are evident, extending to depths of ~10 km in the northwest and to ~4 km in the southeast. High velocity rocks (Vp ~ 6.5 km/s) of the underlying Great Valley ophiolite body are present throughout this part of the section. The section crosses the Garlock Fault (Y ~ -210 km) and the SAF (Y ~ -255 km), where upper and mid-crustal velocities are relatively low (Vp < 6.3 km/s), and then cuts through the San Gabriel Mountains (SGM) and Peninsular Ranges where the upper crust velocities are relatively high (Vp > 6.2 km/s) at shallow depths. Beneath the SAF and SGM, a strong low-velocity zone is apparent, as identified in previous studies in this area, which has been interpreted to indicate fluids (e.g., Ryberg and Fuis, 1998; Fuis et al., 2000).

The section in Figure 7b cuts across the seismically quiet southern San Francisco (SF) Peninsula and SF Bay (X = -120 to -90 km) and then reaches the seismically active Hayward, Calaveras, and Greenville faults beneath the East Bay (X = -70 to -30 km). The section then enters the Great Valley, where the high-velocity basement, thought to be ophiolite (e.g., Godfrey et al., 1997), shallows to the northeast (X = -30 to +50 km). After that, the section enters the Sierra Nevada where a thicker crust with a velocity of ~6.2 km/s extends to 32 km depth. The section in Figure 7c passes through the seismic activity of San Simeon (X = -120 km), Parkfield (X = -75 km), and Coalinga (X = -30 km). Even with the 10 km model gridding, the velocity contrast across the San Andreas at Parkfield is evident (southwest side faster). In this section as well, the high velocity Great Valley ophiolite body is evident with a predominately southwestern dip of its upper surface, consistent with potential field data (Jachens et al., 1995). At X ~ 50 km, we see a transition to the slower, thicker crust of the Sierra Nevada.

S Wave Velocity Model

Although S-wave velocity models in northern California are available from ambient-noise and surface wave data (e.g., Yang et al., 2008), there is no 3D model based on regional data. In this study, we use the first S arrival times from the SCSN and USArray to solve for a Vs model. Figure 8a shows the 1020 SCSN and 1292 USArray events with at least 4 P and 4 S picks. Due to the sparse distribution of the data, we use the velocity inversion nodes of the 3D coarse Vp model (i.e., 30 by 30 km horizontal node spacing). The starting S velocities are derived from our resolved Vp model and a constant Vp/Vs of 1.73. The resolution estimated by the DWS values is quite poor. In order to test the robustness of the S model, we also start with the S velocity values from the ambient noise and teleseismic multiple-plane-wave tomography results by Yang et al. (2008). The well-resolved part agrees with the results starting with the constant Vp/Vs, indicating that the model is relatively robust. Figure 8b shows the map view of our resolved Vs model at 8 km depth. The blue contours enclose the area where the derivative weight sum is greater than 100.

Discussion

Our model is the first 3D seismic velocity model for the entire state of California based on local and regional arrival time data that has ever been developed. It has improved areal coverage compared to the previous northern and southern California models, and extends to greater depth due to the inclusion of substantial data at large epicentral distances. The

combination of northern, southern and central California data sets results in better-resolved velocity structure at the study boundaries of previous tomographic models, such as the San Joaquin Valley and Southern Sierra Nevada. Because of the 10 km horizontal grid spacing in our model inversion, which is larger than the distance cutoff of most waveform cross-correlation calculations (~5 km), we did not apply any differential times from cross-correlation in this study. There may be some finer scale structures that are not resolved due to the data and grid spacing used in our model. We compared our model with some results based on refraction and/or reflection data. Our model generally agrees with most of the studies, such as in the Southern Sierra (Fliedner et al., 1996), the Mojave Desert (Fuis et al., 2001b), the Diablo and Gabilan Ranges (Steppe and Robert, 1978; Walter and Mooney, 1982), the Coyote Lake (Mooney and Luetgert, 1982), the Long Valley (Luetgert and Mooney, 1985), and the San Francisco Bay area (Holbrook et al., 1996); but slightly overestimates near-surface velocity values in some basins and valleys, such as in the greater Los Angeles Basin (Fuis et al., 2001b), the Imperial Valley (McMechan and Mooney, 1980; Fuis et al., 1984), the Great Valley (Colburn and Mooney, 1986), and the Livermore area (Meltzer et al., 1987).

The differences between this statewide velocity model and previous regional-scale models are due to several factors, such as data sets, grid spacing (cell size), tomographic algorithms, and inversion parameters (e.g., damping, smoothing, and residual weighting). The model is very similar to the recent northern California model by Thurber et al. (2009) for the middle to lower crust because the two studies use the same data sets (both absolute and differential times) and inversion algorithm (tomoFDD), whereas the southern California model by Lin et al. (2007) is derived by applying the SIMULPS algorithm (Thurber, 1983, 1993; Eberhart-Phillips, 1990; Evans et al., 1994) to absolute arrival times for composite events. Our new model is generally consistent with these previous results. The improved resolution of our model in near-surface layers over the previous California tomographic models is mainly due to the large amount of active-source data in this study.

The goal of this study is not to replace the previous tomographic models in California that have more detail than can be resolved by our data and grid spacing, but to image the entire state of California at a regional scale, to reveal some features that are difficult to resolve in local studies, and to provide the geophysical community with a velocity model that should be useful for regional-scale studies, such as regional waveform modeling. The model is available through the website http://www.geology.wisc.edu/~glin/STATEWIDE/.

Conclusions

We have developed statewide body-wave tomography models (P and S) for California using absolute and differential arrival times from earthquakes, controlled sources, and quarry blasts. By merging the data sets from networks in northern, southern, and coastal central California and USArray, we have achieved relatively complete coverage of the entire state for Vp. Our model provides a reasonable fit to the data and relocates explosions, treated as earthquakes, with an absolute accuracy of better than a kilometer. Thus it should be useful for producing a statewide earthquake location catalog based on a single velocity model.

References

Begnaud, M. L., K. C. McNally, D. S. Stakes and V. A. Gallardo (2000). A crustal velocity model for locating earthquakes in Monterey Bay, California. Bull. Seismol. Soc. Am., 90, 1391–1408, DOI: 10.1785/0120000016.

Bleibinhaus, F., J. A. Hole, T. Ryberg and G. S. Fuis (2007). Structure of the California Coast Ranges and San Andreas fault at SAFOD from seismic waveform inversion and reflection imaging. J. Geophys. Res., 112, B06315, doi:10.1029/2006JB004611.

Boyd, O. S., C. H. Jones and A. F. Sheehan (2004). Foundering lithosphere imaged beneath the southern Sierra Nevada, California, USA. Science, 305, 660–662.

Brocher, T. M. and D. C. Pope (1994). Onshore-offshore wide-angle seismic recordings of the San Francisco Bay Area Seismic Imaging eXperiment (BASIX); data from the Northern California Seismic Network. U.S. Geol. Surv. Open-File Rept. 94-156.

Brocher, T. M., P. E. Hart and S. Carle (1989). Feasibility study of the seismic reflection method in Amargosa Desert, Nye County, Nevada. U.S. Geol. Surv. Open-File Rept. 89-133, 150 pp.

Brocher, T. M., M. J. Moses and S. D. Lewis (1992). Wide-angle seismic recordings obtained during seismic reflection profiling by the S.P. Lee offshore the Loma Prieta epicenter. U.S. Geol. Surv. Open-File Rept. 92-245, 63 pp.

Catchings, R. D., M. R. Goldman, C. E. Steedman and G. Gandhok (2004). Velocity models, first-arrival travel times, and geometries of 1991 and 1993 USGS land-based controlled-source seismic investigations in the San Francisco Bay Area, California: In-line Shots. U.S. Geol. Surv. Open-File Rept., 2004-1423, 32 pp.

Colburn, R. H. and W. D. Mooney (1986). Two-dimensional velocity structure along the synclinal axis of the Great Valley, California. Bull. Seismol. Soc. Am., 76, 1305–1322.

Colburn, R. H. and A. W. Walter (1984). Data report for two seismic-refraction profiles crossing the epicentral region of the 1983 Coalinga, California earthquakes. U.S. Geol. Surv. Open-File Rept. 84-643, 58 pp.

Eberhart-Phillips, D. (1986). Three-dimensional velocity structure in the northern California Coast Ranges from inversion of local earthquake arrival times. Bull. Seismol. Soc. Am., 76, 1025–1052.

Eberhart-Phillips, D. (1990). Three-dimensional P and S velocity structure in the Coalinga region, California. J. Geophys. Res., 95, 15,343–15,363.

Eberhart-Phillips, D. and A. J. Michael (1993). Three-dimensional velocity structure, seismicity, and fault structure in the Parkfield region, central California. J. Geophys. Res., 98, 15737–15758.

Eberhart-Phillips, D. and A. J. Michael (1998). Seismotectonics of the Loma Prieta, California, region determined from three-dimensional Vp, Vp/Vs, and seismicity. J. Geophys. Res., 103, 21,099–21,120.

Evans, J. R., D. Eberhart-Phillips and C. H. Thurber (1994). User's manual for SIMULPS12 for imaging Vp and Vp/Vs: A derivative of the "Thurber" tomographic inversion SIMUL3 for local earthquakes and explosions. U.S. Geol. Surv. Open-File Rept. 94-431.

Flanagan, M. P., S. C. Myers and K. D. Koper (2007). Regional travel-time uncertainty and seismic location improvement using a three-dimensional a priori velocity model. Bull. Seismol. Soc. Am., 97, 804–825.

Fliedner, M. M., S. Ruppert and the Southern Sierra Nevada Continental Dynamics Working Group (1996). Three-dimensional crustal structure of the southern Sierra Nevada from seismic fan profiles and gravity modeling. Geology, 24, 367–370.

Fliedner, M. M., S. L. Klemperer and N. I. Christensen (2000). Three-dimensional seismic model of the Sierra Nevada arc, California, and its implications for crustal and upper mantle composition. J. Geophys. Res., 105, 10899–10922.

Foxall, W., A. Michelini and T. V. McEvilly (1993). Earthquake travel time tomography of the southern Santa Cruz Mountains: Control of fault rupture by lithological heterogeneity of the San Andreas fault zone. J. Geophys. Res., 98, 17691–17710.

Fuis, G. and W. D. Mooney (1990). Lithospheric structure and tectonics from seismic-refraction and other data. The San Andreas Fault System, California: U.S. Geological Survey Prosessional Paper 1515, chapter 8, 207–236.

D. Mooney, J. H. Healy, G. A. McMechan and W. J. Lutter (1984). A seismic refraction survey of the Imperial Valley region, California. J. Geophys. Res., 89, 1165–1190.

Fuis, G. S., J. J. Zucca, W. D. Mooney and B. Milkereit (1987). A geologic interpretation of seismic-refraction results in northeastern California. Geol. Soc. Am. Bull., 98, 53–65.

Fuis, G. S., T. Ryberg, N. J. Godfrey, D. A. Okaya, W. J. Lutter, J. M. Murphy and V. E. Langenheim (2000). Crustal structure and tectonics of the San Andreas Fault in the Central Transverse Ranges/Mojave Desert Area. 3rd Conference on tectonic problems of the San Andreas Fault System.

Fuis, G. S., J. M. Murphy, D. A. Okaya, R. W. Clayton, P. M. Davis, K. Thygesen, S. A. Baher, T. Ryberg, M. L. Benthien, G. Simila, J. T. Perron, A. K. Yong, L. Reusser, W. J. Lutter, G. Kaip, M. D. Fort, I. Asudeh, R. Sell, J. R. Vanschaack, E. E. Criley, R. Kaderabek, W. M. Kohler and N. H. Magnuski (2001a). Report for borehole explosion data acquired in the 1999 Los Angeles region seismic experiment (LARSE II), southern California. I. Description of the survey. U.S. Geol. Surv. Open-File Rept. 01-408, 82 pp.

Fuis, G. S., T. Ryberg, N. J. Godfrey, D. A. Okaya and J. M. Murphy (2001b). Crustal structure and tectonics from the Los Angeles basin to the Mojave Desert, southern California. Geology, 29, 15–18.

Godfrey, N. J., B. C. Beaudoin and S. L. Klemperer (1997). Ophiolitic basement to the Great Valley forearc basin, California, from seismic and gravity data: Implications for crustal growth at the North American continental margin. Geol. Soc. Am. Bull., 109, 1536–1562.

Hardebeck, J. L., A. J. Michael and T. M. Brocher (2007). Seismic velocity structure and seismotectonics of the eastern San Francisco Bay region, California. Bull. Seismol. Soc. Am., 97, 826–842.

Harris, R., A. W. Walter and G. S. Fuis (1988). Data report for the 1980-1981 seismic-refraction profiles in the western Mojave Desert, California. U.S. Geol. Surv. Open-File Rept. 88-580, 65 pp.

Hauksson, E. (2000). Crustal structure and seismicity distribution adjacent to the Pacific and North America plate boundary in southern California. J. Geophys. Res., 105, 13,875–13,903.

Hauksson, E. and J. S. Haase (1997). Three-dimensional Vp and Vp/Vs velocity models of the Los Angeles basin and central Transverse Ranges, California. J. Geophys. Res., 102, 5423–5453.

Hauksson, E. and J. Unruh (2007). Regional tectonics of the Coso geothermal area along the intracontinental plate boundary in central eastern California: Three-dimensional Vp and Vp/Vs models, spatial-temporal seismicity patterns, and seismogenic deformation. J. Geophys. Res., 112.

Hellweg, M., D. Given, E. Hauksson, D. Neuhauser, D. Oppenheimer and A. Shakal (2007). The California Integrated Seismic Network. Eos Trans. AGU, 88, Jt. Assem. Suppl., Abstract S33C–07.

Henstock, T. J., A. Levander and J. A. Hole (1997). Deformation in the lower crust of the San Andreas Fault System in northern California. Science, 278, 650–653.

Holbrook, W. S., T. M. Brocher, U. S. ten Brink and J. A. Hole (1996). Crustal structure of a transform plate boundary: San Francisco Bay and the central California continental margin. J. Geophys. Res., 101, 22,311–22,334.

Hole, J. A., T. Ryberg, G. S. Fuis, F. Bleibinhaus and A. K. Sharma (2006). Structure of the San Andreas fault zone at SAFOD from a seismic refraction survey. Geophys. Res. Lett., 33, doi:10.1029/2005GL025194.

Huang, J.-l. and D. Zhao (2003). P-wave tomography of crust and upper mantle under southern California: Influence of topography of Moho discontinuity. Acta Seismologica Sinica, 16, 577–587.

Hwang, L. J. and W. D. Mooney (1986). Velocity and Q structure of the Great Valley, California, based on synthetic seismogram modeling of seismic refraction data. Bull. Seismol. Soc. Am., 76, 1053–1067.

Jachens, R. C., A. Griscom and C. W. Roberts (1995). Regional extent of Great Valley basement west of the Great Valley, California: Implications for extensive tectonic wedging in the California Coast Ranges. J. Geophys. Res., 100, 12,769–12,790.

Kohler, W. M. and R. D. Catchings (1994). Data report for the 1993 seismic refraction experiment in the San Francisco Bay Area, California. U.S. Geol. Surv. Open-File Rept. 94-241, 71 pp.

Kohler, W. M. and G. S. Fuis (1988). Data report for the 1979 seismic-refraction experiment in the Imperial Valley region, California. U.S. Geol. Surv. Open-File Rept. 88-255, 96 pp.

Kohler ,W. M., G. S. Fuis and P. A. Berge (1987). Data report for the 1978-1985 seismic-refraction surveys in northeastern California. U.S. Geol. Surv. Open-File Rept. 87-625, 99 pp.

Levander ,A. R., and W. D. Mooney (1987). Upper crustal structure, Livermore Valley and vicinity, California coast ranges. Bull. Seismol. Soc. Am., 77, 1655–1673.

Lin, G., P. M. Shearer, E. Hauksson and C. H. Thurber (2007). A three-dimensional crustal seismic velocity model for southern California from a composite event method. J. Geophys. Res., 112, doi:10.1029/2007JB004977.

Luetgert, J. H. and W. D. Mooney (1985). Crustal refraction profile of the Long Valley caldera, California, from the January 1983 Mammoth Lakes earthquake swarm. Bull. Seismol. Soc. Am., 75, 211–221.

Lutter, W. J., G. S. Fuis, C. H. Thurber and J. Murphy (1999). Tomographic images of the upper crust from the Los Angeles basin to the Mojave Desert, California: Results from the Los Angeles Region Seismic Experiment. J. Geophys. Res., 104, 25,543–25,565.

Lutter,W. J., G. S. Fuis, T. Ryberg, D. A. Okaya, R.W. Clayton, P. M. Davis, C. Prodehl, J. M. Murphy, V. E. Langenheim, M. L. Benthien, N. J. Godfrey, N. I. Christensen, K. Thygesen, C. H. Thurber, G. Simila and G. R. Keller (2004). Upper crustal structure from the Santa Monica Mountains to the Sierra Nevada, Southern Californnia: Tomographic results from the Los Angeles regional seismic experiment, phase II (LARSE II). Bull. Seismol. Soc. Am., 94, 619–632.

Magistrale, H., K. McLaughlin and S. Day (1996). A geology-based 3D velocity model of the Los Angeles Basin Sediments. Bull. Seismol. Soc. Am., 86, 1161–1166.

Manaker, D. M., A. J. Michael and R. Burgmann (2005). Subsurface structure and kinematics of the Calaveras–Hayward fault stepover from three-dimensional Vp and seismicity, San Francisco Bay region, California. Bull. Seismol. Soc. Am., 95, 446–470.

McMechan, G. A. and W. D. Mooney (1980). Asymptotic ray theory and synthetic seismograms for laterally varying structures: theory and application to the Imperial valley, California. Bull. Seismol. Soc. Am., 70, 2021–2035.

Meador, P. J., D. P. Hill and J. H. Luetgert (1985). Data report for the July–August 1983 seismic475 ction experiment in the Mono Craters–Long Valley region, California. U.S. Geol. Surv. Open-File Rept. 85-708, 70 pp.

Mooney, W. D. and R. H. Colburn (1985). A seismic-refraction profile across the San Andreas, Sargent, and Calaveras faults, west-central California. Bull. Seismol. Soc. Am., 75, 175–191.

Mooney, W. D. and J. H. Luetgert (1982). A seismic refraction study of the Santa Clara Valley and southern Santa Cruz Mountains, west-central California. Bull. Seismol. Soc. Am., 72, 901–909. Murphy, J. M. (1989). Data report for the Great Valley, California, axial seismic refraction profiles. U.S. Geol. Surv. Open-File Rept. 89-494, 36 pp.

Murphy, J. M. and A. W. Walter (1984). Data report for a seismic-refraction investigation: Morro Bay to the Sierra Nevada, California. U.S. Geol. Surv. Open-File Rept. 84-642, 37 pp.

Murphy, J. M., R. D. Catchings, W. M. Kohler, G. S. Fuis and D. Eberhart-Phillips (1992). Data report for 1991 active-source seismic profiles in the San Francisco Bay area. U.S. Geol. Surv. Open-File Rept. 92-570, 45 pp.

Murphy, J. M., G. S. Fuis, T. Ryberg, D. A. Okaya, E. E. Criley, M. L. Benthien, M. Alvarez, I. Asudeh, W. M. Kohler, G. N. Glassmoyer, M. C. Robertson and J. Bhowmik (1996). Report for explosion data acquired in the 1994 Los Angeles Region Seismic Experiment (LARSE 94), Los Angeles, California. U.S. Geol. Surv. Open-File Rept. 96-536, 120 pp.

Ryberg, T. and G. S. Fuis (1998). The San Gabriel Mountains bright reflective zone: possible evidence of young mid-crustal thrust faulting in southern California. Tectonophysics, 286, 31–46.

Sharpless, S. W. and A. W. Walter (1988). Data report for the 1986 San Luis Obispo, California, seismic refraction survey. U.S. Geol. Surv. Open-File Rept. 88-35, 48 pp.

Spieth, M. A., D. P. Hill and R. J. Geller (1981). Crustal structure in the northwestern foothills of the Sierra Nevada from seismic refraction experiments. Bull. Seismol. Soc. Am., 71, 1075–1087.

Steppe, A. J. and C. S. Robert (1978). P-velocity models of the southern Diablo Range, California, from inversion of earthquake and explosion arrival times. Bull. Seismol. Soc. Am., 68, 357–367.

Thurber, C. and D. Eberhart-Phillips (1999). Local earthquake tomography with flexible gridding. Comp. Geosci., 25, 809–818.

Thurber, C., S. Roecker, K. Robers, M. Gold, L. Powell and K. Rittger (2003). Earthquake locations and three-dimensional fault zone structure along the creeping section of the San Andreas fault near Parkfield, CA: Preparing for SAFOD. Geophys. Res. Lett., 30, 1112, doi:10.1029/2002GL016004.

Thurber, C., S. Roecker, H. Zhang, S. Baher and W. Ellsworth (2004). Fine-scale structure of the San Andreas fault zone and location of the SAFOD target earthquakes. Geophys. Res. Lett., 31, doi:10.1029/2003GL019398.

Thurber, C., H. Zhang, T. Brocher and V. E. Langenheim (2009). Regional three-dimensional seismic velocity model of the crust and uppermost mantle of northern California. J. Geophys. Res., 114, B01304, doi:10.1029/2008JB005766.

Thurber, C. H. (1983). Earthquake locations and three-dimensional crustal structure in the Coyote Lake area, central California. J. Geophys. Res., 88, 8226–8236.

Thurber, C. H. (1993). Local earthquake tomography: velocities and Vp/Vs-theory. in: Seismic Tomogrphy: Theory and Practice, eds. H. M. Iyer and K. Hirahara, Chapman and Hall, London, 563–583.

Thurber, C. H., S. R. Atre and D. Eberhart-Phillips (1995). Three-dimensional Vp and Vp/Vs structure at Loma Prieta, California, from local earthquake tomography. Geophys. Res. Lett., 22, 3079–3082.

Thurber, C. H., H. Zhang, F. Waldhauser, J. Hardebeck, A. Michael and D. Eberhart-Phillips (2006). Three-dimensional compressional wavespeed model, earthquake relocations, and focal mechanisms for the Parkfield, California, region. Bull. Seismol. Soc. Am., 96, S38–S49.

Thurber, C. H., T. M. Brocher, H. Zhang and V. E. Langenheim (2007). Three-dimensional P wave velocity model for the San Francisco Bay region, California. J. Geophys. Res., 112, doi:10.1029/2006JB004682.

Walter, A. W. and W. D. Mooney (1982). Crustal structure of the Diablo and Gabilan Ranges, central California: A reinterpretation of existing data. Bull. Seismol. Soc. Am., 72, 1567–1590.

Warren, D. (1978). Record sections for two seismic refraction profiles in the Gabilan and Diablo Ranges, California. U.S. Geol. Surv. Open-File Rept. 78-340, 95 pp.

Warren, D. H. (1981). Seismic-refraction measurements of crustal structure near Santa Rosa and Ukiah, California, in Research in the Geysers–Clear Lake geothermal area, northern California. U.S. Geol. Surv. Profess. Pap. 1141, 167–181.

Williams, A. J., T. M. Brocher, W. D. Mooney and A. Boken (1999). Data report for seismic refraction surveys conducted from 1980 to 1982 in the Livermore Valley and the Santa Cruz Mountains, California. U.S. Geol. Surv. Open-File Rept. 99-146, 78 pp.

Yang, Y., M. H. Ritzwoller, F.-C. Lin, M. Moschetti and N. M. Shapiro (2008). Structure of the crust and uppermost mantle beneath the western United States revealed by ambient noise and earthquake tomography. J. Geophys. Res., 113.

Zhang, H. and C. Thurber (2006). Development and applications of double-difference seismic tomography. Pure Appl. Geophys., 163, 373–403.

Zhang, H. and C. H. Thurber (2007). Estimating the model resolution matrix for large seismic tomography problems based on Lanczos bidiagonalization with partial reorthogonalization. Geophys. J. Int., 170, 337–345.

Zhou, H.-W. (2004). Multi-scale tomography for crustal P and S velocities in southern California. Pure Appl. Geophys., 161, 283–302.

Zucca, J. J., G. S. Fuis, B. Milkereit, W. D. Mooney and R. D. Catchings (1986). Crustal structure of northeastern California. J. Geophys. Res., 91, 7359–7382.

Table 1. Previous studies on seismic velocity structure in California.

Study Area	**References**
Coalinga	Eberhart-Phillips (1990)
Coast Ranges	Eberhart-Phillips (1986); Henstock *et al.* (1997); Bleibinhaus *et al.* (2007)
Coso geothermal area	Hauksson and Unruh (2007)
Coyote Lake	Thurber (1983)
Great Valley	Hwang and Mooney (1986); Godfrey *et al.* (1997)
Greater Los Angeles Basin	Magistrale *et al.* (1996); Hauksson and Haase (1997); Lutter *et al.* (1999)
Loma Prieta	Foxall *et al.* (1993); Thurber *et al.* (1995); Eberhart-Phillips and Michael (1998)
Monterey Bay	Begnaud *et al.* (2000)
Parkfield Region	Eberhart-Phillips and Michael (1993); Thurber *et al.* (2003, 2006)
San Francisco Bay Region	Hole *et al.* (2000); Hardebeck *et al.* (2007); Thurber *et al.* (2007)
Santa Monica Mountains	Lutter *et al.* (2004)
Sierra Nevada arc	Brocher *et al.* (1989); Fliedner *et al.* (1996, 2000); Boyd *et al.* (2004)
Entire northern California	Thurber *et al.* (2009)
Entire southern California	Hauksson (2000); Huang and Zhao (2003); Zhou (2004); Lin *et al.* (2007)

Table 2. Active-source data sets included in the statewide tomographic inversion.

Experiment Name	**Reference**	**Year**	**No. Shots**	**No. Stations**
USGS	Warren (1978)	1967	9	147
Geysers-San Pablo Bay	Warren (1981)	1976	5	135
Oroville	Spieth *et al.* (1981)	1977	5	118
Imperial Valley	Kohler and Fuis (1988)	1979	41	932
Western Mojave Desert	Harris *et al.* (1988)	1980	10	245
Gilroy-Coyote Lake	Mooney and Luetgert (1982)	1980/1981	4	236
Livermore	Williams *et al.* (1999)	1980/1981	3	251
Great Valley	Murphy (1989); Colburn and Walter (1984)	1981/1982	7	221
San Juan Bautista	Mooney and Colburn (1985)	1981/1982	6	335
Shasta 1981	Kohler *et al.* (1987)	1981	1	274
Shasta 1982	Kohler *et al.* (1987)	1982	9	299
Morro Bay	Murphy and Walter (1984)	1982	9	230
Coalinga	Murphy and Walter (1984)	1983	9	209
Long Valley	Meador *et al.* (1985)	1983	9	278
San Luis Obispo	Sharpless and Walter (1988)	1986	10	123
Loma Prieta	Brocher *et al.* (1992)	1990	2252	16
San Francisco Bay 1991	Murphy *et al.* (1992); Kohler and Catchings (1994)	1991	6	300
PACE 1992	Fliedner *et al.* (1996)	1992	5	384
Southern Sierra	Fliedner *et al.* (1996)	1993	23	1241
San Francisco Bay 1993	Brocher and Pope (1994); Catchings *et al.* (2004)	1993	14	399
LARSE 1994	Murphy *et al.* (1996)	1994	125	889
LARSE 1999	Fuis *et al.* (2001)	1999	78	925
Parkfield	Thurber *et al.* (2003, 2004); Hole *et al.* (2006)	2003	157	242
Network	Northern and Southern California Earthquake Data Center	1976-2003	270	659

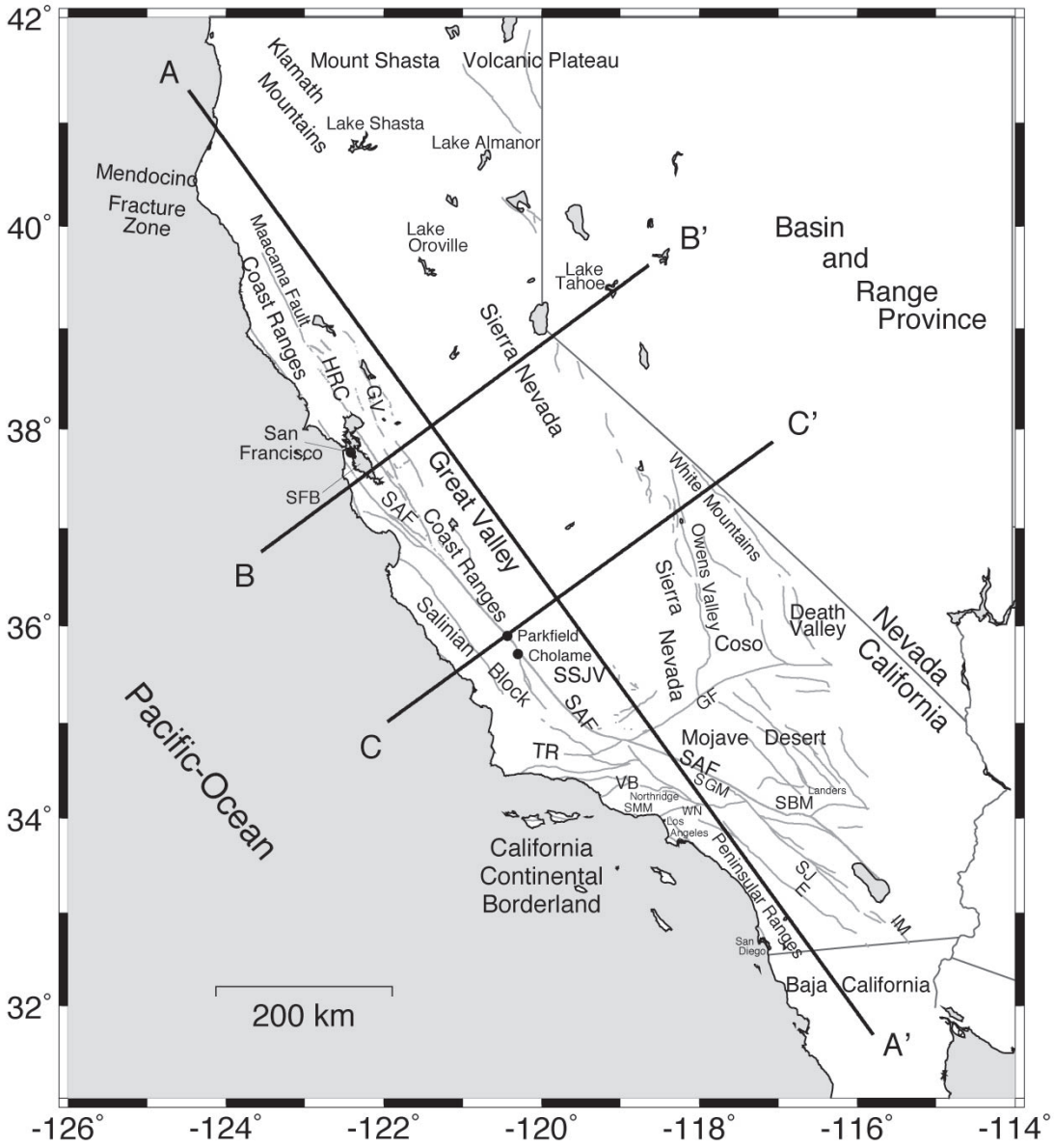

Figure 1. Map of selected geological and geographic features in our study area. The thick straight lines indicate the model cross-sections shown in Figure 7. The NW-SE profile A-A' is parallel to the San Andreas fault, and the SW-NE profiles B-B' and C-C' are perpendicular to the San Andreas fault. Abbreviations are E, Elsinore Fault; GF, Garlock Fault; GV, Green Valley Fault; HRC, Healdsburg-Rodgers Creek Fault; IM, Imperial Valley Fault; SAF, San Andreas Fault; SBM, San Bernardino Mountains; SFB, San Francisco Bay; SGM, San Gabriel Mountains; SJ, San Jacinto Fault; SMM, Santa Monica Mountains; SSJV, Southern San Joaquin Valley; TR, Transverse Ranges; VB, Ventura Basin.

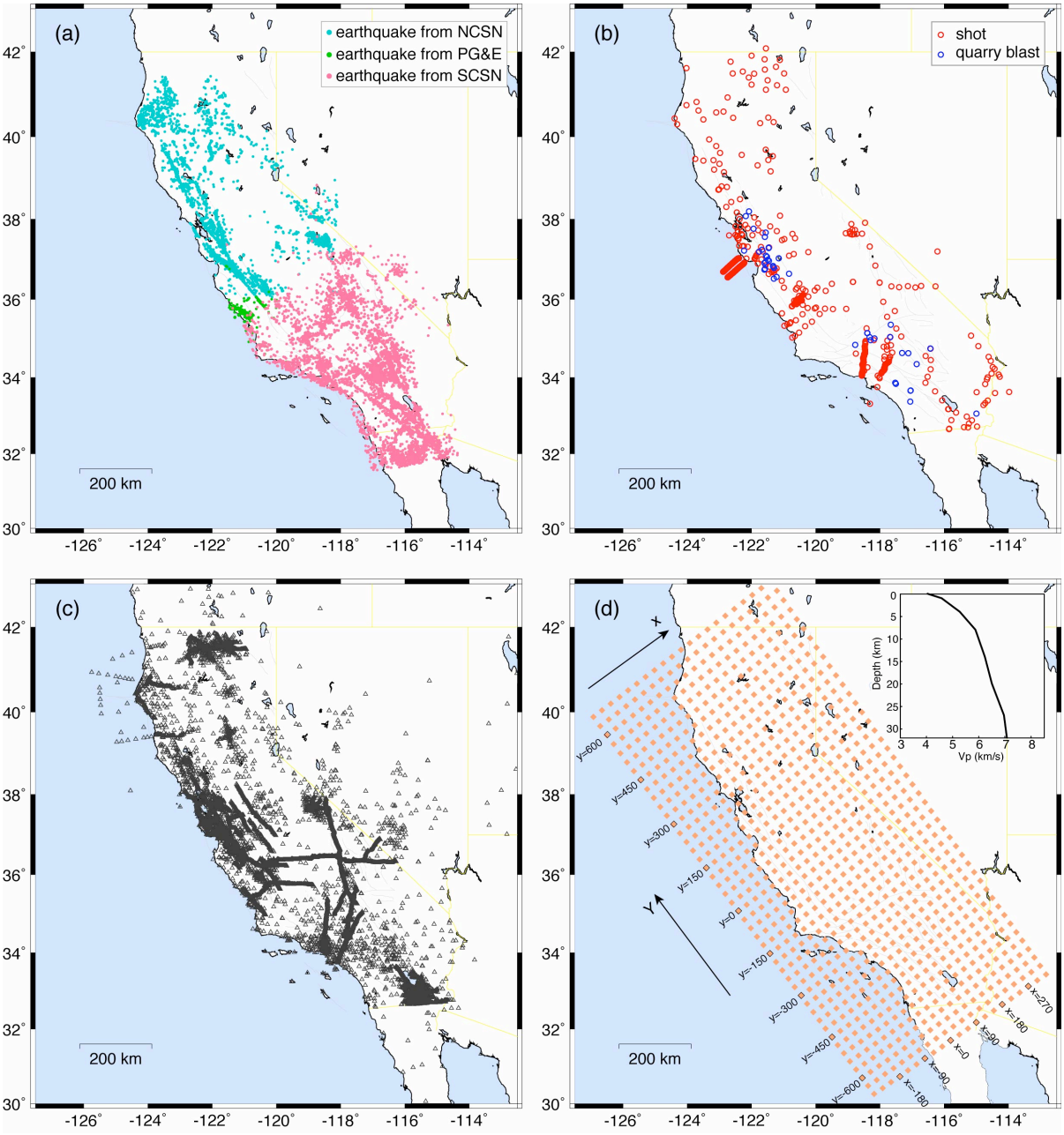

Figure 2. Event and station distributions in our study area and starting inversion grid nodes for the 3D coarse model (30-km horizontal spacing). (a) earthquakes; (b) controlled sources; (c) stations; (d) inversion grid nodes (small panel shows the 1D starting velocity model).

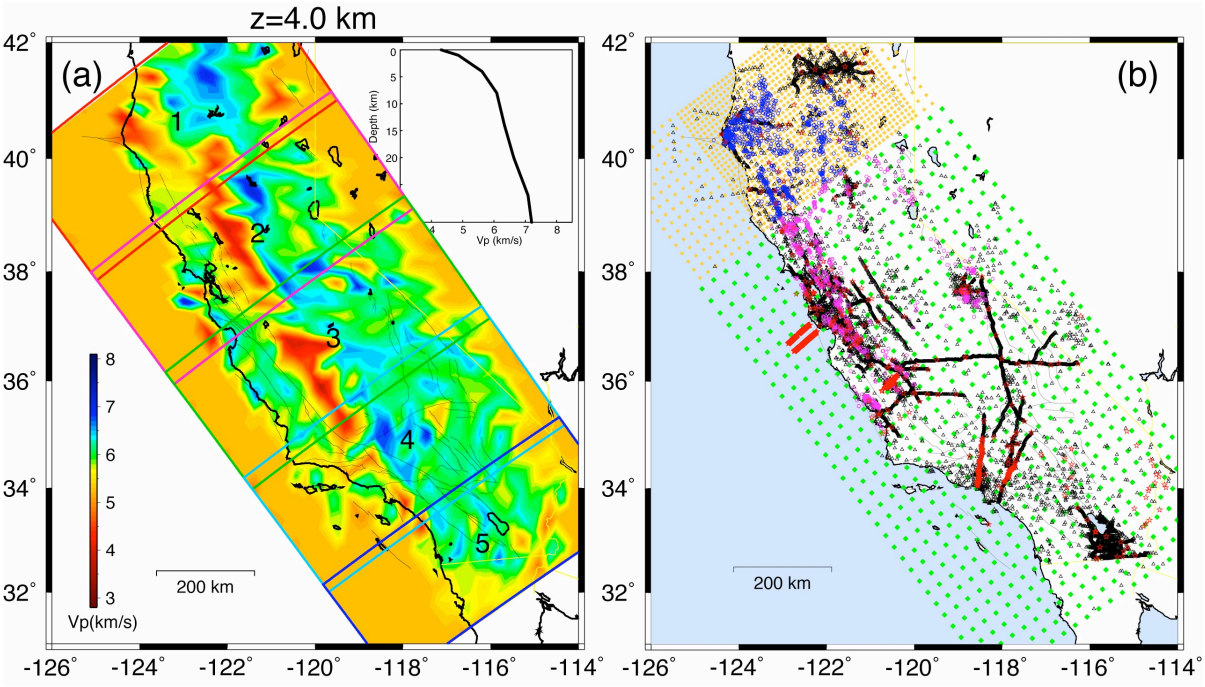

Figure 3. (a) Map view of the 3D coarse velocity model at 4 km depth and the boundaries of the 5 subregions (small panel shows the 1D layer-average velocity). (b) Event and station distribution in the subregion 1. Yellow squares: finer inversion nodes inside of subregion; green squares: nodes with fixed velocities; blue circles: earthquakes inside of subregion 1; pink circles; earthquakes outside of subregion 1 but recorded by stations inside of the subregion; black triangles: permanent and temporary stations; red circles: active sources (shots and quarry blasts). Please refer to the text for more details.

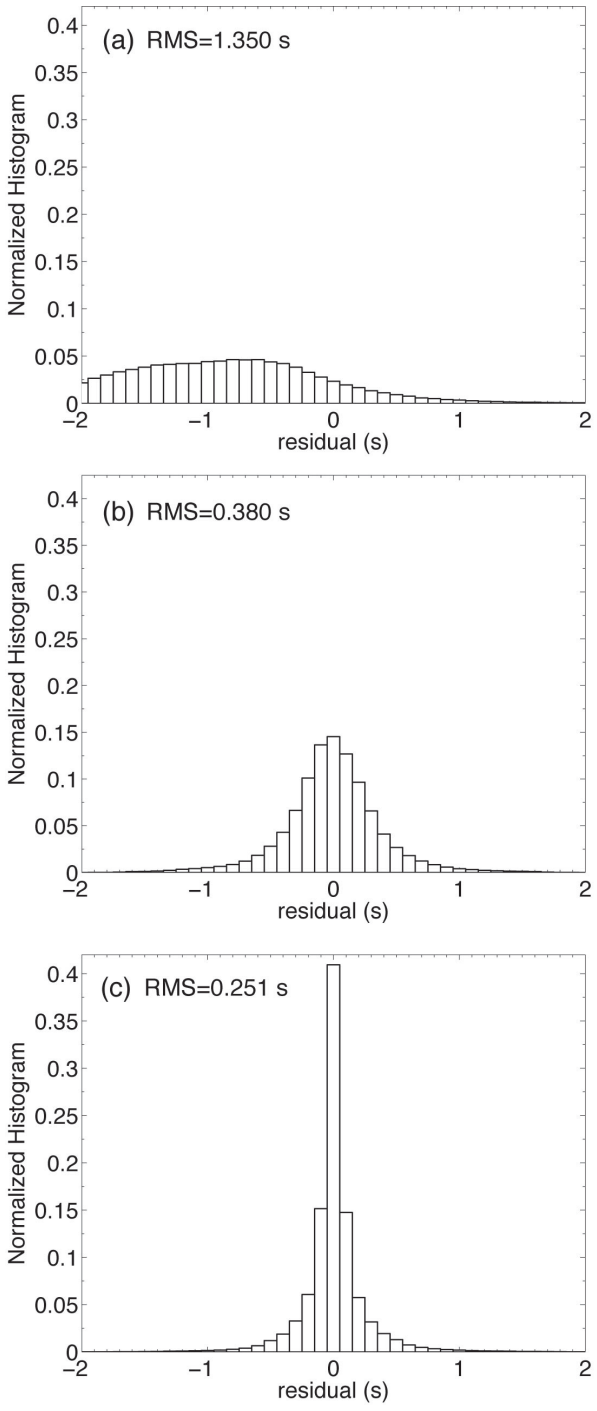

Figure 4. Comparison of the arrival time residual distribution for the entire data set (a) before 3D velocity inversion; (b) after 3D coarse model inversion; (c) after 3D final model inversion.

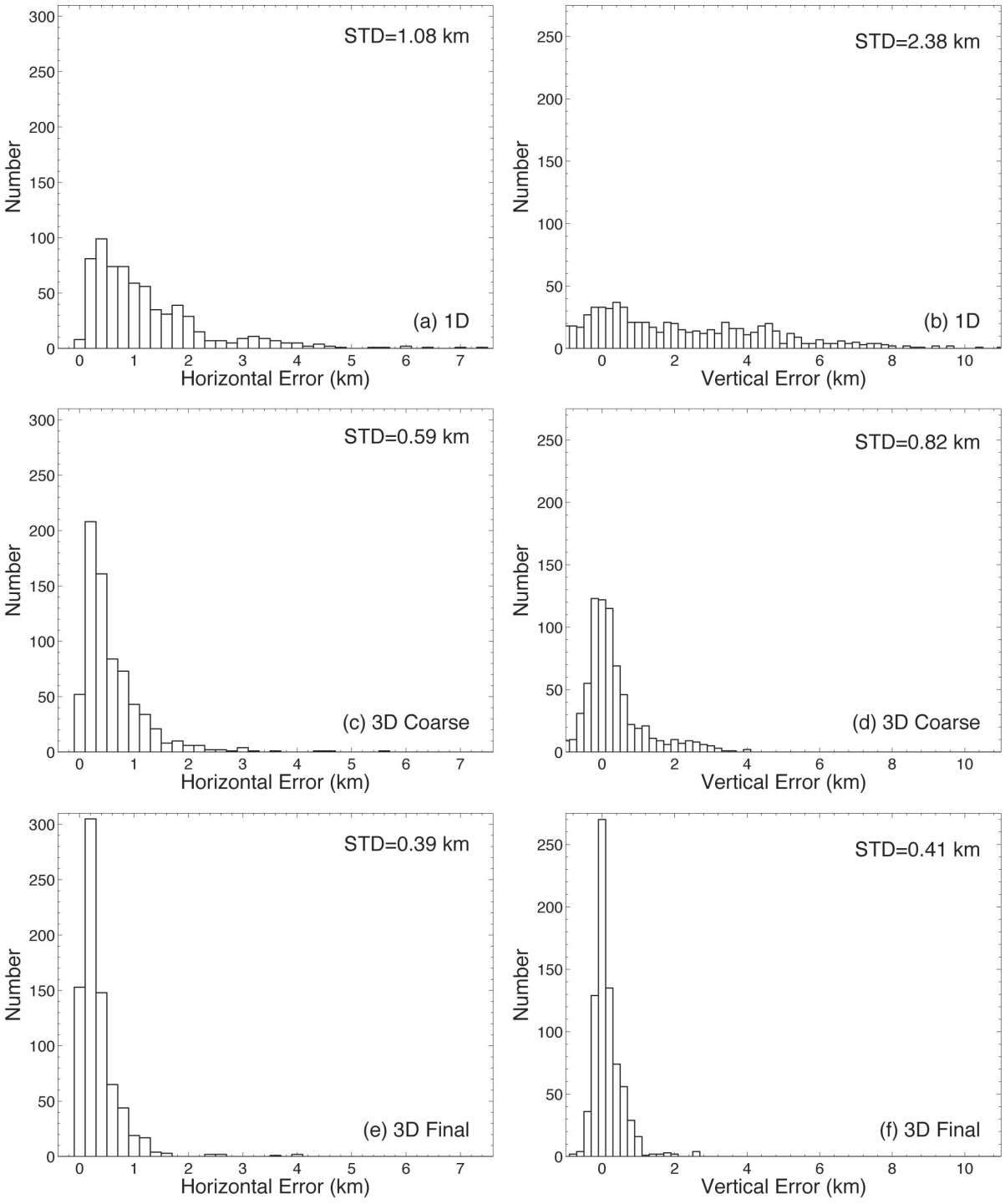

Figure 5. Histograms of the differences between relocations and known true locations for on-land explosions. The two columns are for horizontal and vertical location errors, respectively. (a) and (b) 1D model; (c) and (d) 3D Coarse model; (e) and (f) 3D final model.

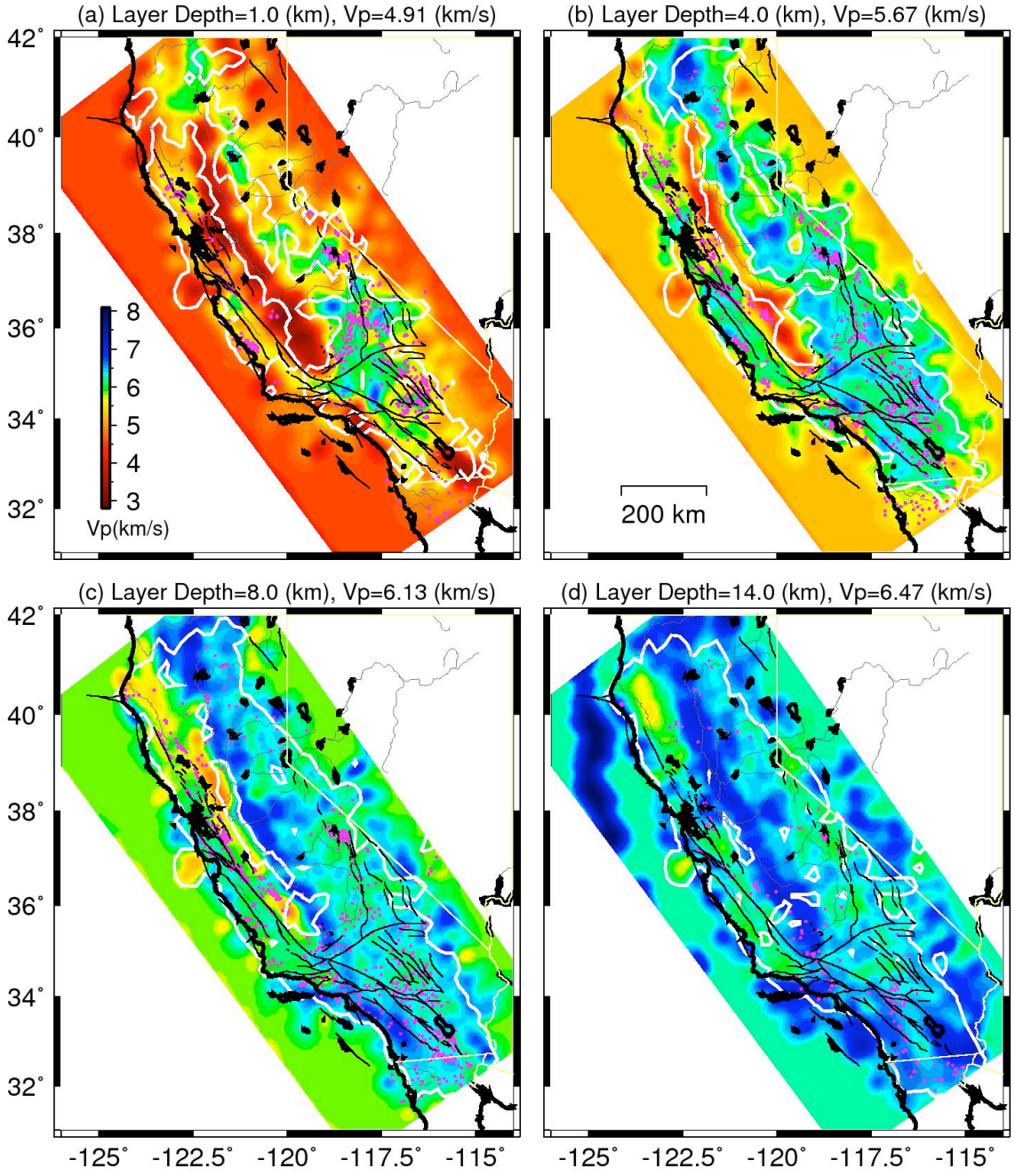
(a) Layer Depth=1.0 (km), Vp=4.91 (km/s)
(b) Layer Depth=4.0 (km), Vp=5.67 (km/s)
(c) Layer Depth=8.0 (km), Vp=6.13 (km/s)
(d) Layer Depth=14.0 (km), Vp=6.47 (km/s)
42˚
40˚
38˚
36˚
34˚
32˚
8
7
6
5
4
3
Vp(km/s)
200 km
-125˚
-122.5˚
-120˚
-117.5˚
-115˚

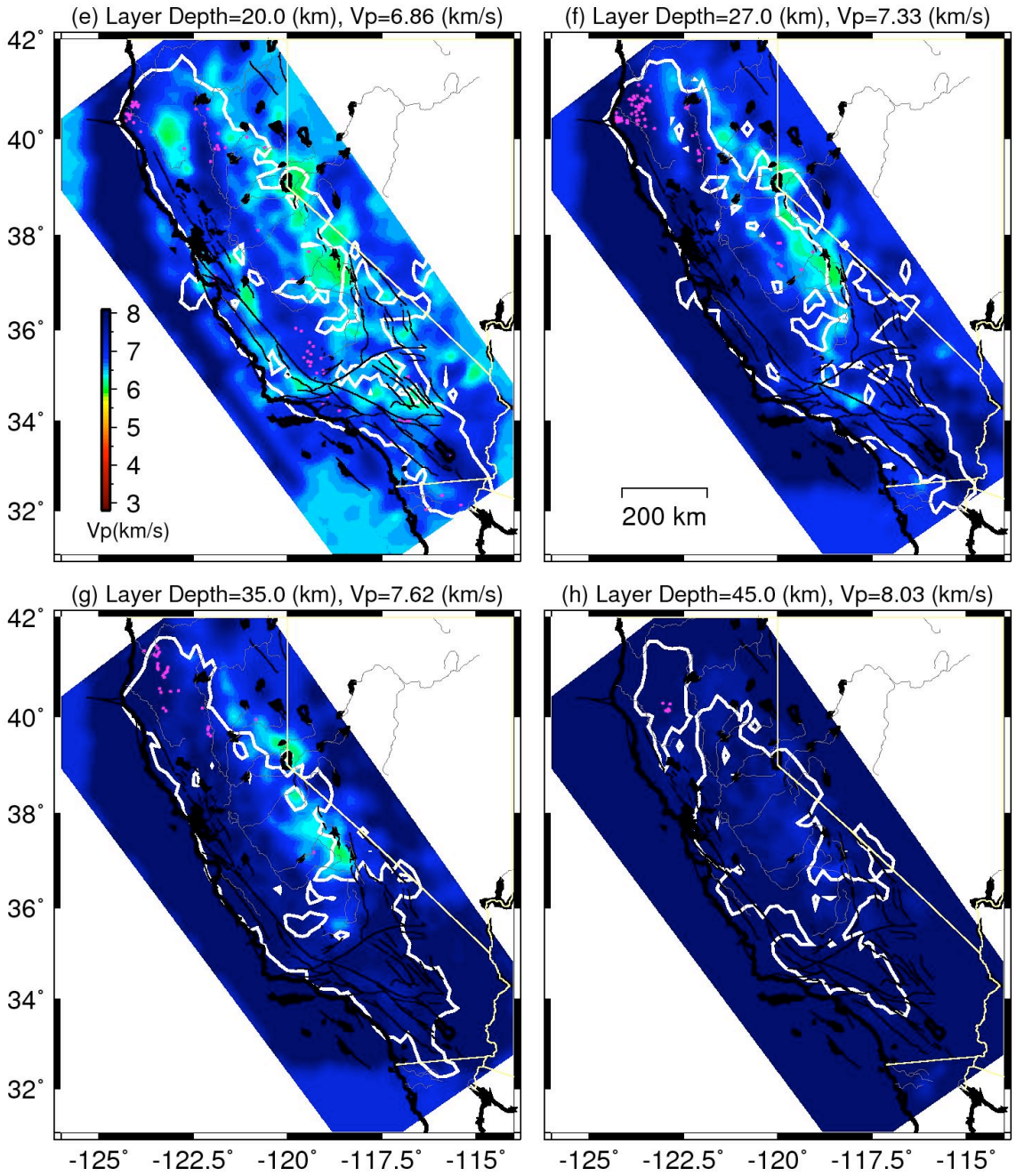

Figure 6. Map views of the P-wave velocity model at different depth slices. Pink dots represent relocated earthquakes. Black lines denote coast line and lakes, gray lines rivers and surface traces of mapped faults. The white contours enclose the areas where the derivative weight sum is greater than 50.

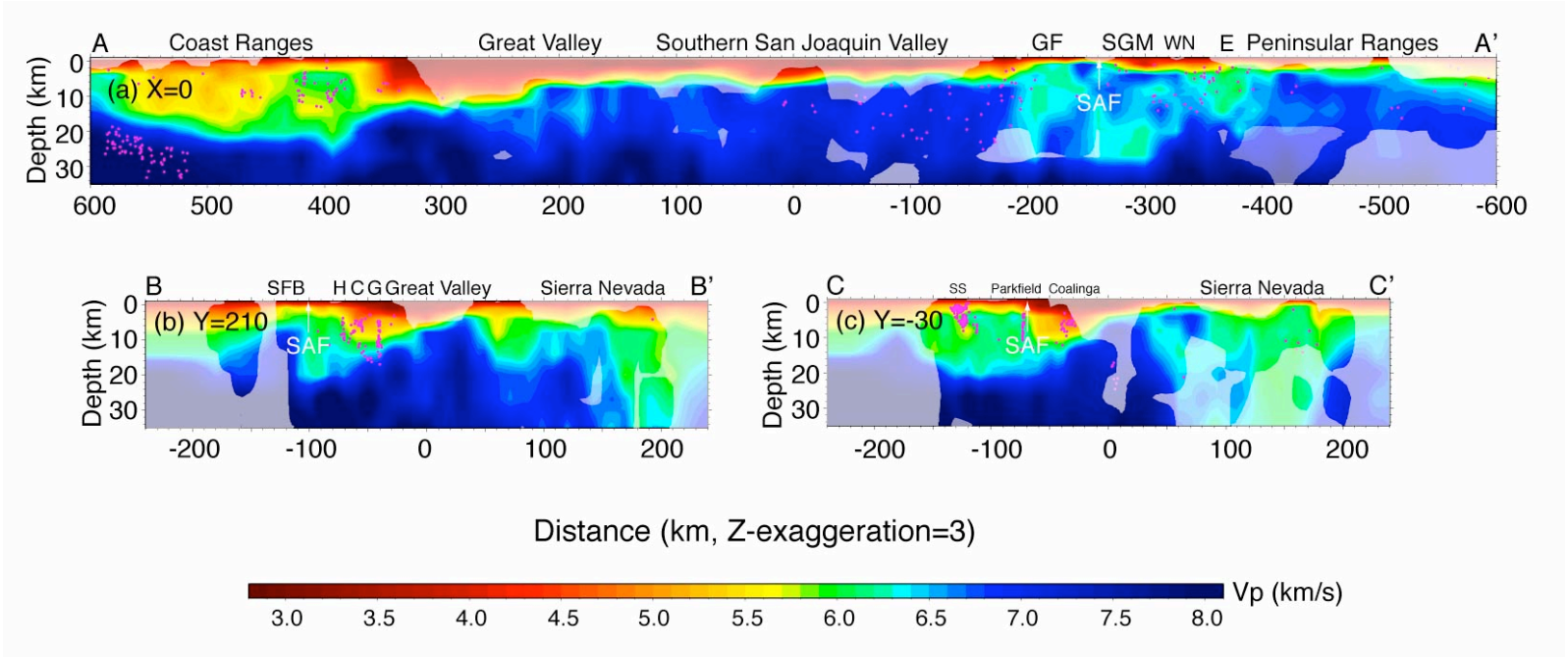

Figure 7. Cross-sections of the absolute P-wave velocity along the three profiles shown in Figure 1. Again, the pink dots represent relocated earthquakes and the parts with masking opacity show the area where the derivative weight sum is less than 50. Abbreviations are C, Calaveras Fault; E, Elsinore Fault; GF, Garlock Fault; G, Greenville Fault; H, Hayward Fault; SAF, San Andreas Fault (shown by the arrows); SFB, San Francisco Bay; SGM, San Gabriel Mountains; SS, San Simeon; WN, Whittier Narrows.

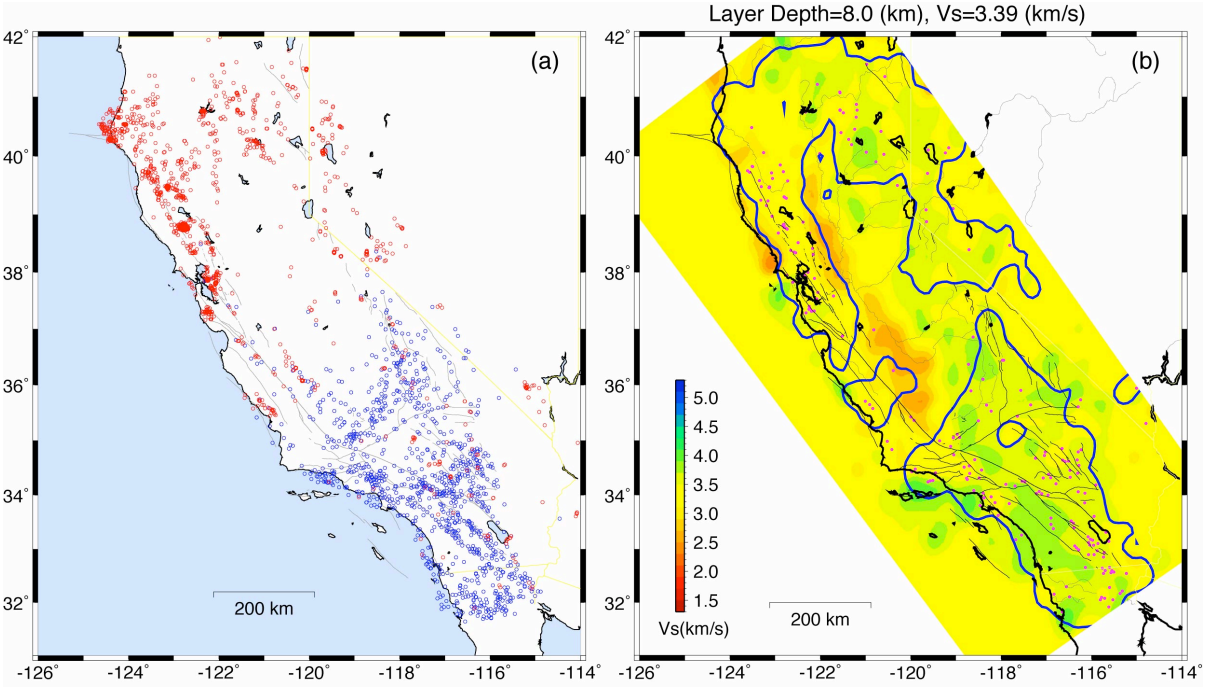

Figure 8. (a) Event distribution for Vs model. The red and blue circles represent the events from the USArray and SCSN, respectively. (b) Map view of our resolved Vs model at 8 km depth. The pink dots represent relocated earthquakes and the blue contours enclose the area where the derivative weight sum is greater than 100.

Bibliography

Brocher, T. M., C. Thurber, H. Zhang, G. Lin, P. Shearer, E. Hauksson, F. Waldhauser, D. Schaff, and J. Hardebeck, 2007, Progress towards a comprehensive crustal seismic velocity model for the State of California, USA, 2nd International Workshop on Long-Period Ground Motion Simulations and Velocity Structures, Earthquake Research Institute, University of Tokyo, Japan, Nov. 2007.

Lin, G., C. Thurber, H. Zhang, E. Hauksson, P. M. Shearer, F. Waldhauser, J. Hardebeck, T. M. Brocher, and D. Schaff, A California statewide three-dimensional seismic velocity model from both absolute and differential times, Fall AGU Meeting, S22A-02, 2008.

Lin, G., P. M. Shearer, E. Hauksson, and C. H. Thurber, A three-dimensional crustal seismic velocity model for southern California from a composite event method, J. Geophys. Res., 112, doi:10.1029/2007JB004,977, 2007.

Thurber, C., Near-regional tomography in California, Workshop on Multi-Resolution 3D Earth Models to Predict Key Observables in Seismic Monitoring and Related Fields, Berkeley, CA, June 6-7, 2007.

Thurber, C., Development of a state-wide California 3-D tomography model from body-wave arrival data, Southern California Earthquake Center Community Velocity Model/Unified Structural Representation Workshop, Palm Springs, CA, June 13, 2007.

Thurber, C., G. Lin, H. Zhang, E. Hauksson, P. Shearer, F. Waldhauser, J. Hardebeck, and T. Brocher, Development of a state-wide 3-D seismic tomography velocity model for California, SCEC Annual Meeting, Palm Springs, CA, September 2007.

Thurber, C., G. Lin, H. Zhang, E. Hauksson, P. Shearer, F. Waldhauser, J. Hardebeck, and T. Brocher, Development of a state-wide 3-D seismic tomography velocity model for California, Fall AGU Meeting, 2007.

Thurber, C., H. Zhang, T. Brocher, and V. Langenheim, Regional three-dimensional seismic velocity model of the crust and uppermost mantle of northern California, J. Geophys. Res., 114, B01304, doi:10.1029/2008JB005766, 2009.